Role of Insulin Receptor Substrate-1 Serine 307 Phosphorylation and Adiponectin in Adipose Tissue Insulin Resistance in Late Pregnancy

Julio Sevillano,* Javier de Castro,* Carlos Bocos, Emilio Herrera, and M. Pilar Ramos

Facultad de Farmacia, Universidad CEU San Pablo, E-28668 Madrid, Spain

Insulin resistance is a hallmark of late pregnancy both in human and rat. Adipose tissue is one of the tissues that most actively contributes to this reduced insulin sensitivity. The aim of the present study was to characterize the molecular mechanisms of insulin resistance in adipose tissue at late pregnancy. To this end, we analyzed the insulin signaling cascade in lumbar adipose tissue of nonpregnant and pregnant (d 20) rats both under basal and insulin-stimulated conditions. We found that the levels of relevant signaling proteins, such as insulin receptor (IR), IR substrate-1 (IRS-1), phosphatidylinositol 3-kinase, 3-phosphoinositide-dependent kinase-1, ERK1/2, and phosphatase and tensin homolog (PTEN) did not change at late pregnancy. However, insulin-stimulated tyrosine phosphorylation of both IR and IRS-1 were significantly decreased, coincident with decreased IRS-1/p85 association and impaired phosphorylation of AKR mouse thymoma viral protooncogene (Akt) and ERK1/2. This impaired activation of IRS-1 occurred together with an increase of IRS-1 phosphorylation at serine 307 and a decrease in adiponectin levels. To corroborate the role of IRS-1 in adipose tissue insulin resistance during pregnancy, we treated pregnant rats with the antidiabetic drug englitazone. Englitazone improved glucose tolerance, and this pharmacological reversal of insulin resistance was paralleled by an increase of adiponectin levels in adipose tissue as well as by a reduction of IRS-1 serine phosphorylation. Furthermore, the impaired insulin-stimulated tyrosine phosphorylation of IRS-1 in adipose tissue of pregnant animals could be restored *ex vivo* by treating isolated adipocytes with adiponectin. Together, our findings support a role for adiponectin and serine phosphorylation of IRS-1 in the modulation of insulin resistance in adipose tissue at late pregnancy. (*Endocrinology* 148: 5933–5942, 2007)

L ATE PREGNANCY IS characterized by the development of insulin resistance in both human (1–3) and rat (4, 5). Decreased insulin responsiveness, which provides adequate glucose and other nutrients for the development of the fetus, might be responsible for several of the metabolic changes taking place during this late stage of gestation (5–7). The molecular mechanisms of insulin resistance during pregnancy are not completely understood. Insulin initiates its metabolic effects, including glucose transport (8, 9), by binding to the α-subunits of its receptor, which causes a conformational change, activating the intrinsic tyrosine kinase activity of the β-subunit of the receptor. This event initiates a cascade of cell-signaling responses, including autophosphorylation of the insulin receptor (IR) and phosphorylation of the IR substrate (IRS) 1–4 proteins (8) that act as docking

proteins for a number of downstream effector molecules bearing the Src homology-2 (Sh2) domain, such as the p85 regulatory subunit of phosphatidylinositol 3-kinase (PI3K) or growth factor receptor-bound protein 2 (Grb2) (10). In particular, tyrosine phosphorylation of IRS-1 permits its association with p85, which in turn activates PI3K. Through this mechanism, insulin signaling is coupled to the activation of the PI3K effector AKR mouse thymoma viral protooncogene (Akt)/protein kinase B (PKB), a putative mediator of the effects of insulin on glucose transport (11, 12). On the other hand, tyrosine-phosphorylated IRS-1 binds to Grb2, thereby activating the Ras/MAPK pathway, which triggers most of the transcriptional and mitogenic effects of insulin. In addition to tyrosine phosphorylation, the IR and IRS proteins are susceptible to serine phosphorylation, an event that attenuates insulin signaling (13–17).

The question of whether the impaired action of insulin in adipose tissue during pregnancy is due to an impaired binding of insulin to its receptor or, alternatively, occurs at the postreceptor level, is a matter of ongoing debate. Although some investigators did not find any change, or even an increase, in binding of insulin to its receptor (18) and IR number (19), others report a decrease in IR number (20). Previous studies, performed in rat and in obese women, show that both phosphorylation and expression of IRS-1 are diminished at late pregnancy (21–23). Although the impact of impaired IRS-1 signaling on other proteins of the insulin signaling cascade, such as IRS-2 or Akt, has not been explored, these data suggest that insulin resistance of adipose tissue at

late pregnancy may take place at the postreceptor level, similar to what has been reported for other situations of insulin resistance such as obesity or type 2 diabetes (24).

The present study was designed to shed light on the molecular mechanisms underlying the insulin resistance state of adipose tissue at late pregnancy. To this end, we compared levels of insulin signaling proteins in adipose tissue of virgin and pregnant rats at 20 d of gestation and explored insulin-stimulated phosphorylation of IR and IRS-1 in these tissues. These experiments revealed that in adipose tissue of late pregnant rats, there is an increased phosphorylation of IRS-1 at serine 307 and that this event may be involved in the establishment of reduced glucose tolerance in these animals. In addition, we treated pregnant rats with englitazone and show that this antidiabetic drug restored impaired insulin responsiveness in adipose tissue, which was paralleled by an increase of adiponectin levels in adipose tissue as well as by a reduction of IRS-1 serine 307 phosphorylation. Furthermore, the impaired insulin-stimulated tyrosine phosphorylation of IRS-1 in adipose tissue of pregnant animals could be restored *ex vivo* by treating isolated adipocytes with adiponectin. Together, these findings point to a role for adiponectin and IRS-1 serine phosphorylation in the modulation of insulin resistance in adipose tissue at late pregnancy.

Materials and Methods

Animals and sample collection

Female Sprague Dawley rats were housed at 22–24 C with 12-h light cycles (0800–2000 h) and free access to water and chow diet (Panlab, Barcelona, Spain). Animals were mated when they weighed between 180 and 210 g. Day zero of pregnancy was determined by the presence of spermatozoids in vaginal smears. Experimental groups were composed by short-term fasted (4–6 h) virgin rats and rats at 20 d of gestation. After CO_2 anesthesia, animals were decapitated, and lumbar adipose pads were rapidly dissected and either placed in liquid nitrogen and stored at −80 C until further analysis or immediately placed in 0.9% NaCl at 30 C for collagenase preparation of primary adipocytes (see *Isolation of adipocytes and incubation with adiponectin* below). Blood was collected from the neck wound in EDTA tubes for immediate separation of plasma at 4 C. The experimental protocol was approved by the Animal Research Committee of the Faculty of Pharmacy, University CEU San Pablo (Madrid, Spain).

Insulin treatment for insulin signaling studies

For *in vivo* stimulation of the insulin signaling cascade, 16-h fasted nonpregnant and 20-d pregnant rats were anesthetized with sodium pentobarbital (40 mg/kg body weight ip). After the abdominal cavity was opened, saline (0.9% NaCl) with or without insulin (4 IU Humulin NPH/kg body weight; Lilly, Madrid, Spain) was injected via the portal vein. After 90 sec, lumbar adipose tissue was removed, placed in liquid nitrogen, and stored at −80 C.

Englitazone treatment

Englitazone (kindly supplied by Pfizer, Groton, CT) was suspended in 2% Tween 80. Starting at d 16 of gestation, rats were treated daily at 0900 h by oral gavage of a single dose of 50 mg englitazone/kg body weight or vehicle (2% Tween 80). On the morning of d 20 of pregnancy, rats were killed as described above.

Plasma analysis and estimates of insulin resistance

Enzymatic colorimetric tests were used to determine in EDTA-plasma samples glucose (GOD-PAP, from Roche Diagnostics, Barcelona, Spain), triglycerides (LPL/GPO-Trinder from Roche Diagnostics), glycerol

(GPO-Trinder; Sigma-Aldrich, Madrid, Spain), and nonesterified fatty acids (NEFA) (ACS-ACOD; Wako Chemicals GmbH, Neuss, Germany). Insulin (detection limit 0.07 μg/liter, 1.8% intraassay variation, 3.2% interassay variation) and adiponectin (detection limit 50 pg/ml, 4.0% intraassay variation, 6,4% interassay variation) were determined in plasma samples using a specific enzyme immunoassay (EIA) kit for rats (Mercodia, Uppsala, Denmark, and Komed Co., Ltd., Sungnam City, Kyunggi-Do, Korea, respectively). From the short-term fasting plasma glucose and insulin values, the following indexes were calculated as estimates of insulin sensitivity: homeostasis model assessment of insulin resistance (HOMA-IR), quantitative insulin sensitivity check index (QUICKI), and fasting glucose to insulin ratio (FGIR). Recently, we have validated the use of these indexes in rats by comparison with the hyperinsulinemic-euglycemic clamp technique (unpublished results). The HOMA-IR was calculated as the product of the fasting plasma glucose (FPG) and insulin (FPI) divided by a constant, assuming that control young adults rats have an average HOMA-IR of 1, analogous to the assumptions applied in the development of HOMA-IR in humans (25). The equation was as follows HOMA-IR = (FPG × FPI)/2430, FPI was in micro-units per milliliter and FPG in milligrams per deciliter. The QUICKI was calculated according to the original formula (26) as the inverse log sum of fasting insulin in micro-units per milliliter and fasting glucose in milligrams per deciliter. QUICKI = 1/[log(FPG) + log(FPI)]. Finally, the FGIR was calculated as the ratio of fasting plasma glucose divided by fasting plasma insulin (27). FGIR = FPG/FPI, where FPG was in milligrams per deciliter and FPI in micro-units per milliliter.

Oral glucose tolerance tests (OGTT)

Where indicated, 20-d pregnant control and englitazone-treated-rats were subjected to an OGTT in fasted conditions (16 h fasting). After a basal blood sample from the tail vein was drawn, a bolus of glucose (2 g/kg) was administered orally to the animals. Subsequently, blood samples were collected into EDTA tubes at 7.5, 15, 20, 30, 45, and 60 min after glucose administration and placed on ice. Subsequently, samples were centrifuged, and plasma was stored at −20 C until processed for glucose and insulin determinations as described above. The areas under the curve for glucose and insulin were calculated using the Kaleida-Graph software package (version 4.03; Synergy Software, Reading, PA).

Materials for immunodetection and immunoprecipitation

For immunoprecipitation and immunodetection by Western blot, the following antibodies were used: monoclonal anti-phosphotyrosine (PY20) from Transduction Laboratories (Lexington, KY); rabbit anti-IR-β antibodies from Santa Cruz Biotechnology (Santa Cruz, CA); rabbit polyclonal antibodies against IRS-1, IRS-2, phospho-IRS-1 (Ser307), p85 subunit of PI3K, ERK1/2, and sheep polyclonal Akt (recognizes Akt-1, Akt-2, and Akt-3 isoforms) from Upstate Biotechnology (Lake Placid, NY); anti-PTEN and anti-PDK rabbit polyclonal antibodies from Cell Signaling Technology (Beverly, MA); rabbit polyclonal antiadiponectin from Chemicon (Temecula, CA); rabbit polyclonal anti-phospho-IRS-1 (Tyr612) and monoclonal anti-β-actin antibodies from Sigma-Aldrich; and total Akt (sensitivity <0.1 ng/ml, 7.7% intraassay variation, 9.3% interassay variation) and Ser-473/Thr-308 phosphorylated Akt (sensitivity <0.8 U/ml, 6.8% intraassay variation, 8.3% interassay variation) ELISA kits and phospho-Tyr187/Thr185 ERK1/2 antibodies from Biosource International (Camarillo, CA). Protein A/G-agarose was from Santa Cruz Biotechnology. All other reagents for immunoblotting were from standard suppliers (Sigma-Aldrich or Amersham Biosciences, Barcelona, Spain).

Immunoprecipitation

For immunoprecipitation, 800 mg frozen adipose tissue was lysed in an ice-cold RIPA buffer containing 30 mm HEPES (pH 7.4), 5 mm EDTA, 1% Nonidet P-40, 1% Triton X-100, 0.5% sodium deoxycholate, 8 mm Na_3VO_4, 1 mm NaF, and 2 mm protease inhibitor (Pefablock; Roche). Tissue homogenates were incubated with anti-IR or IRS-1 antibodies for 2 h at 4 C, followed by incubation with protein A/G-agarose for another 2 h at 4 C. Immunoprecipitates were separated using spin-collection filters (Cytosignal, Irvine, CA) and washed once with RIPA buffer (0.15 mm NaCl, 10 mm phosphate, 1% Nonidet P-40, 0.5% sodium deoxy-

cholate, 0.1% SDS) and three times with PBS. Immunoprecipitated proteins were eluted from the spin-collection filters by addition of 40 μl Laemmli buffer [0.125 M Tris-HCl (pH 6.8), 4% SDS, 10% 2-mercaptoethanol, 20% glycerol, 0.02% bromphenol blue].

Protein extraction and immunoblotting

Frozen lumbar adipose tissue (200 mg) was powdered in liquid nitrogen using a mortar precooled to -80 C and lysed by incubation for 30 min in an ice-cold 30 mM HEPES buffer (pH 7.4) containing 5 mM EDTA, 1% Triton X-100, 0.5% sodium deoxycholate, and 2 mM protease inhibitor (Pefablock; Roche). Cellular debris was pelleted by centrifugation at $17,000 \times g$ for 30 min at 4 C. The supernatant was collected, and protein concentration was determined using the bicinchoninic acid protein assay from Pierce (Rockford, IL).

Twenty-five micrograms of protein extract from each experimental condition or, where indicated, immunoprecipitates were subjected to SDS-PAGE and electrotransferred to polyvinylidene difluoride membranes. Membranes were blocked for 1 h at room temperature with 5% nonfat dry milk or, for the detection of tyrosine-phosphorylated proteins, with 2.5% BSA. Membranes were incubated at 4 C overnight with the indicated antibodies. After washing, the membranes were incubated at room temperature with either antimouse or antirabbit horseradish peroxidase-conjugated secondary antibodies as appropriate. To quantify tyrosine-phosphorylated IR or IRS-1 in the immunoprecipitates, membranes were incubated overnight at 4 C with a primary antibody against phosphotyrosine, conjugated with horseradish peroxidase (PY20). To analyze PI3K association with IRS-1, coimmunoprecipitation of p85 regulatory subunit of PI3K was detected by immunodetection with anti-PI3K p85 antibody in the IRS-1 immunoprecipitates. Immunoreactive bands were visualized using the enhanced chemiluminescence system and quantified by densitometry. The intensity of each protein was corrected by the values obtained from the immunodetection of β-actin.

Isolation of adipocytes and incubation with adiponectin

Adipocytes were prepared from white lumbar adipose tissue of 20-d pregnant rats as described previously (7). Briefly, freshly isolated adipose pads were digested with collagenase A (1 mg/ml) (Roche; activity 0.21 U/mg) in Krebs-Ringer bicarbonate (KRB) buffer (pH 7.4) containing 4% (wt/vol) BSA (fatty acid free, fraction V; Sigma-Aldrich) and 5.5 mM glucose for 30 min at 37 C in an O_2/CO_2 atmosphere (19:1, vol/vol) under constant shaking (60 cycles/min). After filtering and washing with KRB buffer to eliminate collagenase, cells were resuspended in the same buffer at a concentration of about 0.5×10^6 cells/ml, and 0.25 ml of the adipocyte suspension was incubated for 30 min in the absence or presence of 1 μg adiponectin/ml (recombinant rat gAcrp30; Biovision Research, Mountain View, CA). Subsequently, cells were incubated for another 5 min in the absence or presence of 100 nM insulin. Then, cells were lysed in an ice-cold RIPA buffer containing 30 mM HEPES (pH 7.4),

5 mM EDTA, 1% Nonidet P-40, 1% Triton X-100, 0.5% sodium deoxycholate, 8 mM Na_3VO_4, 1 mM NaF, and 2 mM protease inhibitor (Pefablock; Roche) and processed for the analysis of tyrosine phosphorylation of IRS-1 by Western blot as described in *Protein extraction and immunoblotting*.

Phosphotyrosine phosphatase activity

Phosphotyrosine phosphatase activity was determined in homogenates from adipose tissue, using the protein tyrosine phosphatase assay kit (Sigma-Aldrich), following the instructions of the manufacturer.

Expression of the results and statistical evaluation

Results are expressed as mean $\pm$ SEM of four to 17 animals per group. Regarding the log-normal distribution of the insulin concentration, the statistical analyses were done on the logarithm of this parameter. As indicated in table and figure legends, statistical comparisons between two groups were made with the Student's *t* test and between three or more groups by ANOVA with 95% confidence limits.

Results and Discussion

Changes of body weight and metabolic parameters at late pregnancy

As shown in Table 1, both lumbar adipose tissue and maternal body weight increased at late pregnancy and, as expected, late pregnant rats (d 20) had significantly lower plasma glucose levels in the presence of hyperinsulinemia (Table 1). Plasma concentrations of triglycerides, glycerol, and NEFA in the 20-d pregnant rats were significantly higher than those in nonpregnant animals, confirming the well known hyperlipemia and enhanced adipose tissue lipolytic activity at late pregnancy (28). The significantly higher HOMA-IR as well as the significantly lower QUICKI and FGIR indexes in the 20-d pregnant animals compared with nonpregnant rats (Table 1) further confirmed the insulin-resistant state associated with late pregnancy. Together, these data reflect the characteristic metabolic changes at late pregnancy (29). As also shown in Table 1, circulating plasma adiponectin was significantly lower in late pregnant than virgin rats.

TABLE 1. Effect of late pregnancy on body and adipose tissue weight and on biochemical parameters and insulin sensitivity indexes

	Virgin rats	20-d pregnant rats	P
Body weight (g)	223.5 ± 4.7 (n = 12)	340.0 ± 7.9 (n = 9)	<0.001
Lumbar adipose tissue weight (g)	1.21 ± 0.10 (n = 8)	2.04 ± 0.20 (n = 7)	0.002
Plasma glucose (mg/dl)	125.9 ± 6.5 (n = 9)	93.5 ± 10.2 (n = 6)	0.014
Plasma insulin (μg/liter)	0.85 ± 0.16 (n = 8)	2.17 ± 0.62 (n = 7)	0.012
Plasma triglycerides (mg/dl)	83.5 ± 10.1 (n = 8)	267.7 ± 33.1 (n = 7)	<0.001
Plasma glycerol (μM)	281.1 ± 22.9 (n = 9)	552.9 ± 48.6 (n = 6)	<0.001
Plasma NEFA (μM)	562.1 ± 68.9 (n = 8)	1299.6 ± 150.9 (n = 8)	<0.001
Plasma adiponectin (μg/ml)	18.3 ± 0.9 (n = 5)	14.6 ± 1.2 (n = 5)	0.046
HOMA-IR	0.97 ± 0.29 (n = 6)	2.07 ± 0.36 (n = 5)	0.040
QUICKI	0.305 ± 0.009 (n = 6)	0.272 ± 0.008 (n = 5)	0.033
FGIR (mg/10^{-4} U)	7.80 ± 1.49 (n = 6)	2.23 ± 0.67 (n = 5)	0.011

Enzymatic colorimetric tests were used to determine in EDTA-plasma samples glucose (GOD-PAP; Roche), triglycerides (LPL/GPO-Trinder; Roche), glycerol (GPO-Trinder; Sigma-Aldrich), and NEFA (ACS-ACOD; Wako). Insulin and adiponectin were determined in plasma samples using a specific EIA kit for rats (Mercodia and Komed, respectively). Insulin sensitivity indexes HOMA-IR, QUICKI, and FGIR were calculated from short-term fasting plasma glucose and insulin values as described in *Materials and Methods*. Data are mean values $\pm$ SEM. Values of plasma insulin were log-transformed to equalize the variance between conditions. Comparisons were made by Student's *t* test for unpaired data with equal or unequal variance as appropriate.
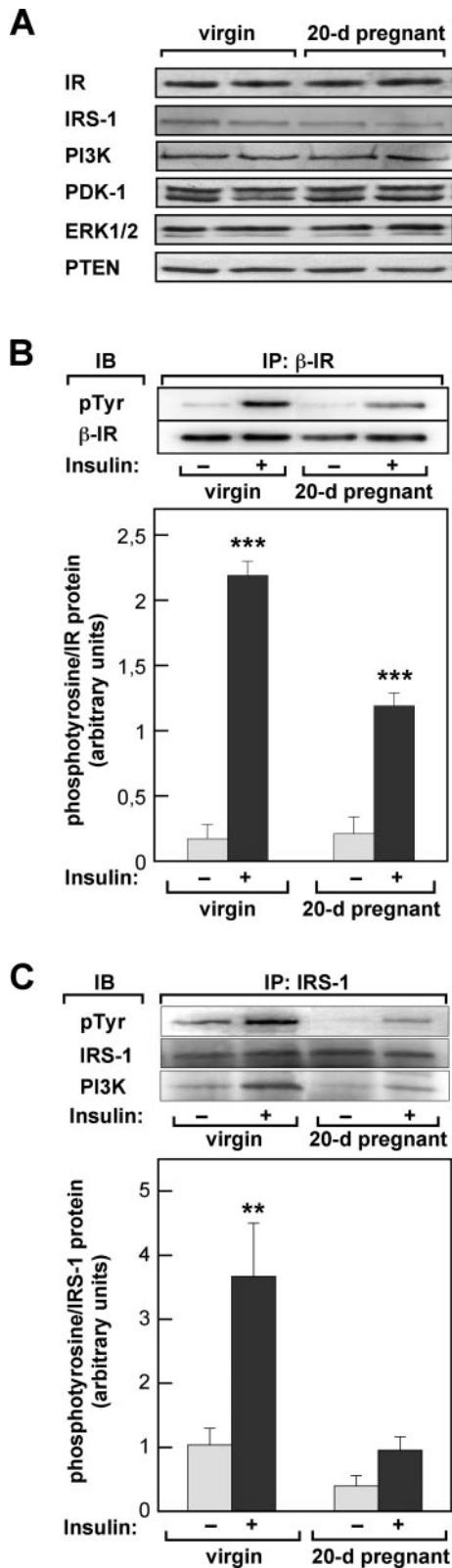
Insulin-stimulated tyrosine phosphorylation of IR and IRS-1 are impaired in adipose tissue of late pregnant rats

It is well known that insulin resistance develops in adipose tissue at late pregnancy. To further investigate the molecular changes underlying impaired insulin signaling at late gestation, we analyzed the expression of some cardinal proteins of the insulin signaling cascade in lumbar adipose tissue. Western blot analysis revealed that there was no difference in the total amount of the signaling proteins IR, IRS-1, PI3K, 3-phosphoinositide-dependent kinase-1 (PDK-1), ERK1/2 (or p42/p44 MAPK), and phosphatase and tensin homolog (PTEN) in 20-d pregnant rats as compared with nonpregnant animals (Fig. 1A). These data fit well with the observation that the amount of IR protein does not change in the skeletal muscle of pregnant women (30) and support the hypothesis that, similar to other situations of insulin resistance like obesity or type 2 diabetes (24), postbinding receptor defects play a major role on development of peripheral insulin resistance at late pregnancy.

Upon binding to its receptor, insulin induces the activation and autophosphorylation of the IR. We analyzed whether decreased IR phosphorylation was involved in the blunted response of adipose tissue to insulin in late pregnant animals. To this end, virgin and 20-d pregnant rats were treated iv with insulin or saline, and homogenates of the lumbar adipose tissue were immunoprecipitated with anti-IR antibodies. As shown in Fig. 1B, upon *in vivo* stimulation with insulin, IR became significantly tyrosine phosphorylated in both groups of animals. However, insulin-stimulated IR phosphorylation was much higher in adipose tissue from virgin than from 20-d pregnant rats (12.9 ± 0.6-fold and 5.7 ± 0.6-fold for virgin and 20-d pregnant animals, respectively, $P < 0.001$).

Tyrosine phosphorylation of the IR is a prerequisite for the recruitment and subsequent phosphorylation of IRS-1. Pre-

ern blot analysis of IR, IRS-1, PI3K, PDK-1, ERK1/2, and PTEN in the adipose tissue homogenates reveals that there is no difference in the total amount of these cardinal proteins of the insulin signaling cascade at late gestation. B and C, Insulin-stimulated phosphorylation of the IR (B) as well as IRS-1 levels and association of IRS-1 with PI3K (C) in the adipose tissue of nonpregnant and late pregnant rats. After 16 h fasting, virgin and 20-d pregnant rats were anesthetized with sodium pentobarbital (40 mg/kg body weight ip), and then saline (0.9% NaCl) (*light gray bars*) or insulin (4 IU Humulin NPH/kg body weight) (*dark gray bars*) was injected via the portal vein. After 90 sec, lumbar adipose tissue was removed, and after lysis in ice-cold RIPA buffer containing 30 mM HEPES (pH 7.4), 5 mM EDTA, 1% Nonidet P-40, 1% Triton X-100, 0.5% sodium deoxycholate, 8 mM Na$_3$VO$_4$, 1 mM NaF, and 2 mM protease inhibitor (Pefablock), tissue homogenates were incubated with anti-β-subunit of the IR (B) or IRS-1 antibodies (C) for 2 h at 4 C, followed by incubation with protein A/G-agarose for another 2 h at 4 C. Immunoprecipitated proteins were subjected to Western blot analysis and immunodetected with anti-phosphotyrosine antibodies (pTyr) and then with anti-IR or -IRS-1 antibodies. Association of PI3K with IRS-1 was monitored by coimmunoprecipitation experiments, detecting the p85 regulatory subunit of PI3K by Western blot in IRS-1 immunoprecipitates (C). Representative immunoblots (IB) for phosphorylated and total proteins as well as for coimmunoprecipitated PI3K are shown above the graphs. The graphs show the levels of tyrosine-phosphorylated IR (B) and IRS-1 (C) normalized to the total amount of IR and IRS-1 protein, respectively, of five (IR) or four (IRS-1) independent experiments. **, $P < 0.01$; ***, $P < 0.001$ for insulin- *vs.* saline-treated animals.

Fig. 1. Insulin-stimulated-tyrosine phosphorylation of IR and IRS-1 are impaired in the adipose tissue of late pregnant rats. A, Immunodetection of insulin signaling proteins. Lumbar adipose tissue of virgin and 20-d pregnant rats was homogenized in an ice-cold 30 mM HEPES buffer (pH 7.4) containing 5 mM EDTA, 1% Triton X-100, 0.5% sodium deoxycholate, and 2 mM protease inhibitor (Pefablock). West-

vious studies in skeletal muscle of both obese women and rats show that IRS-1 phosphorylation is diminished at late pregnancy (21–23), suggesting a main role of IRS-1 regulation in the insulin resistance state. To explore the role of IRS-1 in the blunted response of adipose tissue to insulin in late
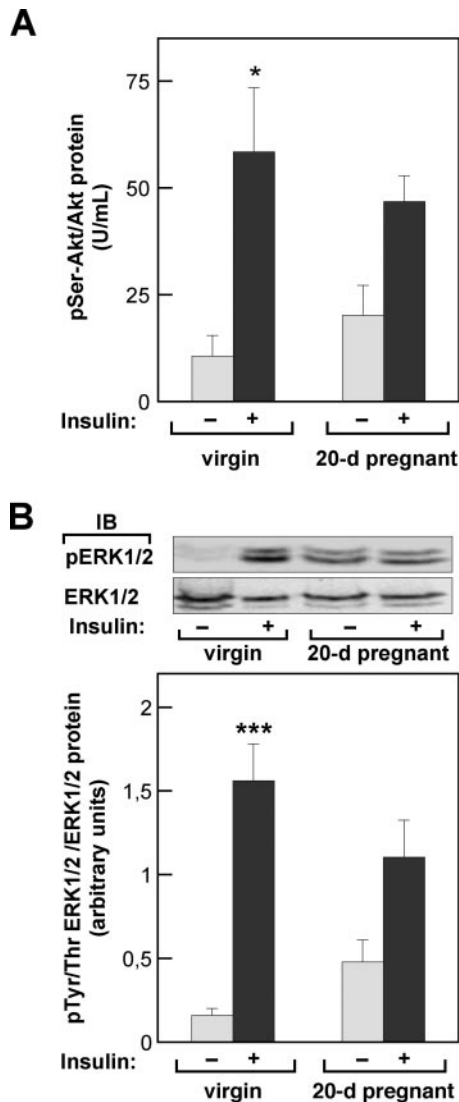

A

B

FIG. 2. Insulin-stimulated phosphorylation of Akt and ERK1/2 are impaired in the adipose tissue of late pregnant rats. After 16 h fasting, virgin and 20-d pregnant rats were anesthetized with sodium pentobarbital (40 mg/kg body weight ip), and then saline (0.9% NaCl) (*light gray bars*) or insulin (4 IU Humulin NPH/kg body weight) (*dark gray bars*) was injected via the portal vein. After 90 sec, lumbar adipose tissue was removed and lysed in an ice-cold 30 mM HEPES buffer (pH 7.4) containing 5 mM EDTA, 1% Triton X-100, 0.5% sodium deoxycholate, and 2 mM protease inhibitor (Pefablock). A, Total Akt and Ser-473/Thr-308-phosphorylated Akt were quantified by ELISA kits in the adipose tissue homogenates. The graph shows the levels of phosphorylated Akt, normalized to the total amount of Akt protein, of three independent experiments performed in duplicate. B, Phospho-Tyr187/Thr185 ERK1/2 and ERK1/2 were immunodetected by Western blot analysis in adipose tissue homogenates. The graph shows the levels of phosphorylated ERK1/2, normalized to the total amount of ERK1/2 protein, of three independent experiments. A representative immunoblot (IB) for phosphorylated and total protein is shown above the graph. *, $P < 0.05$; ***, $P < 0.001$ for insulin- *vs.* saline-treated animals.

pregnant animals, we determined the amount of tyrosine-phosphorylated IRS-1 in virgin and 20-d pregnant rats that had been acutely treated with insulin or saline. As shown in Fig. 1C, although tyrosine phosphorylation of IRS-1 was stimulated almost 4-fold by insulin in adipose tissue of non-pregnant animals ($P < 0.01$), insulin did not induce any significant phosphorylation of IRS-1 in the 20-d pregnant rats ($P = 0.1$). Together, these data show that insulin-stimulated tyrosine phosphorylation of both IR and IRS-1 is greatly impaired in adipose tissue at late pregnancy.

Once activated by tyrosine phosphorylation, IRS-1 serves as a docking protein for downstream effector molecules. In particular, p85 binding to tyrosine-phosphorylated IRS-1 stimulates PI3K. To confirm the impact of impaired tyrosine phosphorylation of IR and IRS-1 on the insulin signaling cascade, we next analyzed PI3K (p85 subunit) association with IRS-1 by immunodetection of p85 in adipose tissue extracts that had been immunoprecipitated previously with anti-IRS-1. As shown in Fig. 1C (*inset*), upon stimulation with insulin, a band with the expected molecular mass of the regulatory subunit of PI3K (85 kDa) was detected in the IRS-1 immunoprecipitates of both groups of animals, pointing to the formation of a stable complex between IRS-1 and PI3K. Of note, the amount of this complex was more than 2-fold lower in the 20-d pregnant rats compared with nonpregnant animals, supporting the notion that decreased tyrosine phosphorylation of IRS-1 in adipose tissue of pregnant rats in fact impairs insulin signaling in this tissue.

We next analyzed Akt/PKB, an enzyme downstream of PI3K, which is known to mediate a number of metabolic and mitogenic actions of insulin (10). In response to insulin, Akt
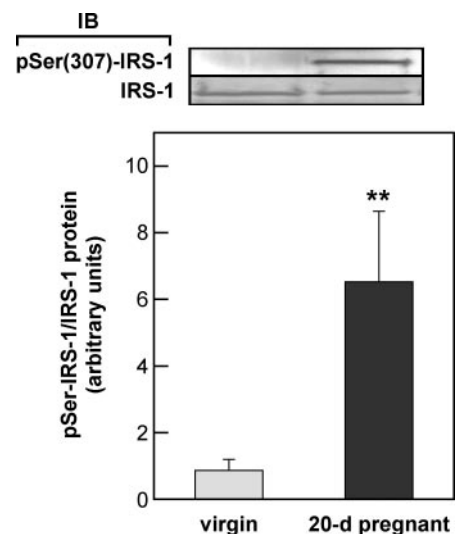

FIG. 3. Serine 307 phosphorylation of IRS-1 is increased in adipose tissue at late gestation. Lumbar adipose tissue of virgin and 20-d pregnant rats was homogenized in an ice-cold 30 mM HEPES buffer (pH 7.4) containing 5 mM EDTA, 1% Triton X-100, 0.5% sodium deoxycholate, and 2 mM protease inhibitor (Pefablock). Phospho-IRS-1 (Ser307) and IRS-1 were immunodetected by Western blot analysis in adipose tissue homogenates. The graph shows the levels of serine 307-phosphorylated IRS-1, normalized to the total amount of IRS-1 protein, of five virgin and four 20-d pregnant rats. A representative immunoblot (IB) for phosphorylated and total protein is shown above the graph. **, $P < 0.01$, pregnant *vs.* nonpregnant animals.

becomes activated by serine phosphorylation (31). We found that, in line with the reduction observed in insulin-stimulated tyrosine phosphorylation of IR and IRS-1 protein (see above), insulin significantly stimulated serine phosphorylation of Akt in adipose tissue of virgin rats but had only a minor and nonsignificant effect on Akt phosphorylation in pregnant animals (Fig. 2A). Similarly, we found that insulin significantly stimulated tyrosine/threonine phosphorylation of the ERK1/2 in adipose tissue of virgin rats but failed to induce significant changes in late pregnant rats (Fig. 2B). These data indicate that impaired IR and IRS-1 tyrosine phosphorylation are hallmarks of the insulin resistance state in adipose tissue during late gestation.

Serine 307 phosphorylation of IRS-1 is increased in adipose tissue at late gestation

One mechanism that may account for decreased tyrosine phosphorylation of IRS-1 is the activation of protein tyrosine phosphatases (PTPs), such as PTP1B, which would result in the rapid dephosphorylation of IRS-1 (32). However, we did not detect any increment of phosphotyrosine phosphatase activity in the adipose tissue of late pregnant rats compared with nonpregnant animals (12.7 ± 3.3 and 10.3 ± 1.2 nmol phosphate/mg protein·min for virgin and 20-d pregnant rats, respectively, $P > 0.1$), thus excluding PTPs as negative regulators of insulin signaling in our experimental system.

Alternatively, IRS-1 activation may be impaired through inhibitory modifications of the protein, such as the phosphorylation of serine residues, in particular serine 307, which is known to ablate the ability of IRS-1 to activate downstream PI3K-dependent pathways (33). Here, we analyzed the serine 307 phosphorylation state of IRS-1 in virgin and late pregnant rats. As shown in Fig. 3, serine phosphorylation of IRS-1 at serine 307 was markedly higher (~7-fold, $P < 0.001$) in adipose tissue of late pregnant rats compared with virgin controls. These data implicate, for the first time, increased serine 307 phosphorylation of IRS-1 in insulin resistance in adipose tissue during pregnancy. Interestingly, serine phosphorylation of IRS-1 has also been observed in other conditions of insulin resistance, such as obesity (34) and type 2 diabetes (10, 35). IRS-1 contains numerous serine/threonine phosphorylation sites in amino acid sequence motifs, including serine 307 analyzed in the present study. This amino acid is potentially recognized by different kinases, including protein kinase C (PKC), c-Jun-N-terminal kinase (JNK), mammalian target of rapamycin (mTOR), or inhibitor of κ-light polypeptide gene enhancer in B cells, kinase β (IKKβ) (36). The question of whether one or several of these kinases are involved in the IRS-1 serine phosphorylation in adipose tissue at late pregnancy remains to be investigated.

Pharmacological reversal of insulin resistance at late pregnancy is paralleled by decreased IRS-1 serine 307 phosphorylation in adipose tissue

To confirm the role of serine 307-phosphorylated IRS-1 in the modulation of insulin responsiveness during pregnancy, we established a model of reversal of insulin resistance. To this end, pregnant rats were treated from d 16–20 of gestation with the antidiabetic drug englitazone. Englitazone belongs to the class of thiazolidinediones (TZDs) that act as ligands of peroxisome proliferator-activated receptor γ (PPARγ). These drugs are known insulin sensitizers, and they are clinically used in oral antidiabetic therapy (37). As shown in Table 2, maternal body weight was unaffected by the treatment, although a reduction in the lumbar adipose tissue weight was observed. Importantly, englitazone-treated animals exhibited a marked reduction of maternal hyperlipidemia, as evidenced by a significant decrease of triglycerides, glycerol, and NEFA (Table 2). In addition, the treated animals had significantly lower insulin concentrations in the presence of normoglycemia and had significantly higher plasma adiponectin concentrations, values similar to those of the nonpregnant condition (Table 1). To further investigate the insulin-glucose relationships after treatment with englitazone, an OGTT was performed. Figure 4, A and C, shows the glucose and insulin curves during the OGTT in the control and englitazone-treated pregnant rats. Pregnant rats that had been treated with englitazone clearly showed a lower glucose

TABLE 2. Effects of englitazone (EZ) treatment on body and adipose tissue weight, biochemical parameters, and insulin sensitivity indexes in 20-d pregnant rats

	Control pregnant rats	EZ-treated pregnant rats	P
Body weight (g)	351.0 ± 5.4 (n = 11)	346.6 ± 4.7 (n = 8)	NS
Lumbar adipose tissue weight (g)	2.23 ± 0.15 (n = 13)	1.74 ± 0.09 (n = 11)	0.015
Plasma glucose (mg/dl)	108.0 ± 3.9 (n = 17)	104.7 ± 4.9 (n = 10)	NS
Plasma insulin (μg/liter)	1.66 ± 0.16 (n = 19)	0.89 ± 0.12 (n = 12)	0.002
Plasma triglycerides (mg/dl)	268.3 ± 28.9 (n = 10)	87.5 ± 15.1 (n = 7)	<0.001
Plasma glycerol (μM)	630.3 ± 58.2 (n = 13)	374.2 ± 34.4 (n = 9)	0.003
Plasma NEFA (μM)	1082.2 ± 128.8 (n = 17)	650.0 ± 94.6 (n = 9)	0.03
Plasma adiponectin (μg/ml)	15.8 ± 0.8 (n = 11)	19.7 ± 1.0 (n = 10)	0.008
HOMA-IR	1.89 ± 0.23 (n = 14)	0.99 ± 0.21 (n = 8)	0.016
QUICKI	0.276 ± 0.004 (n = 14)	0.304 ± 0.009 (n = 8)	0.018
FGIR (mg/10^{-4} U)	3.01 ± 0.30 (n = 14)	5.44 ± 2.62 (n = 8)	0.037

From d 16 of gestation, rats were treated daily, by oral gavage, with a dose of 50 mg englitazone (kindly supply by Pfizer) suspended in 2% Tween 80/kg body weight, or vehicle (2% Tween 80). On the morning of the 20th day of pregnancy, animals were killed and blood collected in EDTA-containing tubes. Enzymatic colorimetric tests were used to determine in EDTA-plasma samples glucose (GOD-PAP; Roche), triglycerides (LPL/GPO-Trinder; Roche), glycerol (GPO-Trinder; Sigma-Aldrich), and NEFA (ACS-ACOD; Wako). Insulin and adiponectin were determined in plasma samples using a specific EIA kit for rats (Mercodia and Komed, respectively). Insulin sensitivity indexes HOMA-IR, QUICKI, and FGIR were calculated from short-term fasting plasma glucose and insulin values as described in *Materials and Methods*. Data are mean values ± SEM. Values of plasma insulin were log-transformed to equalize the variance between conditions. Comparisons were made by Student's *t* test for unpaired data with equal or unequal variance as appropriate.

and insulin increase after the oral glucose load. Thus, the areas under the curves for both glucose (Fig. 4B) and insulin (Fig. 4D) were significantly lower (more than a 50% decrease) in the englitazone-treated animals. These findings, together with decreased HOMA-IR and increased QUICKI and FGIR indexes (Table 2), indicate that englitazone treatment in late pregnant rat reverses their insulin-resistant condition.

Although the detailed mechanisms of TDZ-mediated insulin sensitization are still unclear, there is increasing evidence that these drugs exert their insulin-sensitizing effects, at least in part, by activating (38) or modulating the expression (39) of proteins of the insulin signaling cascade. We therefore analyzed the insulin signaling proteins in the adipose tissue of englitazone-treated animals. As shown in Fig. 5A, we did not detect any change of the total amount of IR,

FIG. 5. Englitazone decreases IRS-1 serine 307 phosphorylation in adipose tissue of late pregnant rats. From d 16 of gestation, rats were treated daily, by oral gavage, with a dose of 50 mg englitazone (kindly supplied by Pfizer) suspended in 2% Tween 80/kg body weight or vehicle (2% Tween 80). On the morning of the 20th day of pregnancy, animals were killed, and adipose tissue was dissected and subsequently homogenized in an ice-cold 30 mM HEPES buffer (pH 7.4), containing 5 mM EDTA, 1% Triton X-100, 0.5% sodium deoxycholate, and 2 mM protease inhibitor (Pefablock) for Western blot analysis. A, Immunodetection of insulin signaling proteins. Western blot analysis of IR, IRS-1, IRS-2, PI3K, PDK-1, Akt, ERK1/2, and PTEN in the adipose tissue homogenates reveals that englitazone does not affect the total amount of these cardinal proteins of the insulin signaling cascade at late gestation; B, phospho-IRS-1 (Ser307) and IRS-1 were immunodetected by Western blot analysis in the adipose tissue homogenates of control (*gray bar*) and englitazone-treated (*black bar*) 20-d pregnant rats. The graph shows the levels of serine 307-phosphorylated IRS-1 protein, normalized to the total amount of IRS-1, of seven control and five englitazone-treated 20-d pregnant rats. A representative immunoblot (IB) for phosphorylated and total protein is shown above the graph. *, $P < 0.05$, englitazone-treated *vs.* untreated control animals.
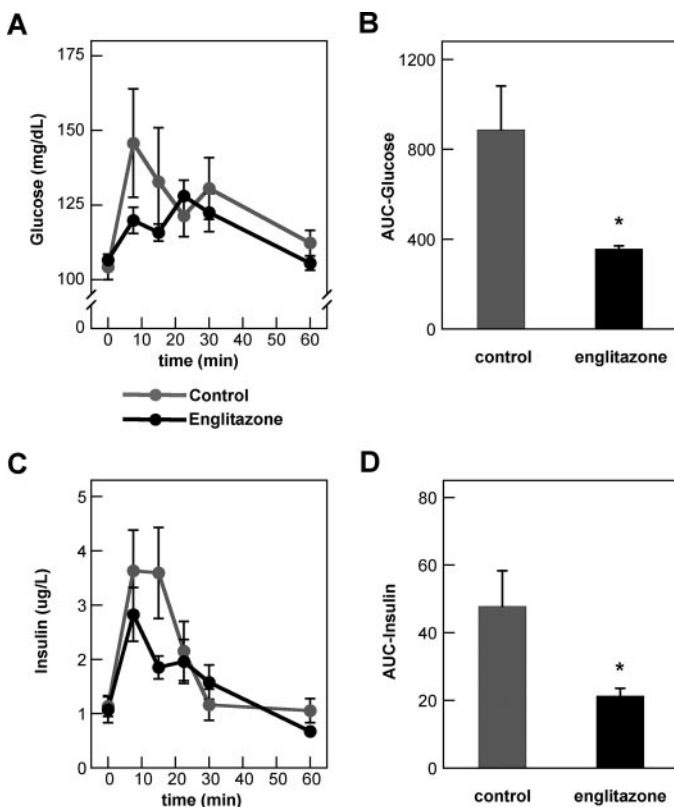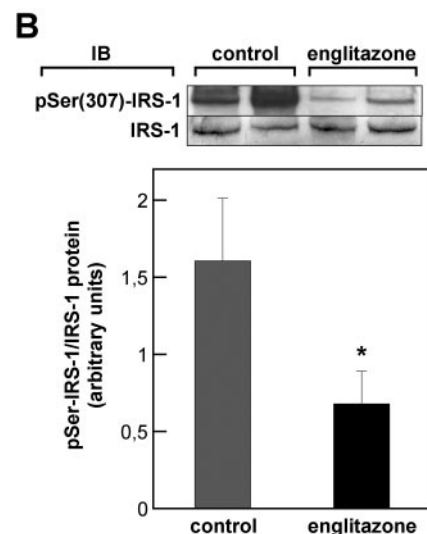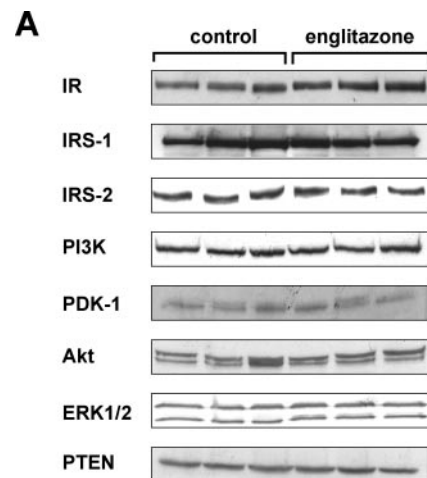
FIG. 4. Englitazone improves insulin resistance of late pregnant rats. From d 16 of gestation, rats were treated daily, by oral gavage, with one dose of 50 mg englitazone (kindly supplied by Pfizer) suspended in 2% Tween 80/kg body weight or vehicle (2% Tween 80). On the morning of the 20th day of pregnancy, animals were subjected to an OGTT in fasted conditions (16 h fasting). After a basal blood sample from the tail vein was drawn, a bolus of glucose (2 g/kg) was administered orally to the animals. Subsequently, blood samples were collected at 7.5, 15, 20, 30, 45, and 60 min after glucose administration, and after the plasma analysis of glucose and insulin was performed, the area under the curve for both parameters was calculated. A, Plasma glucose of control (*gray circles*) and englitazone-treated (*black circles*) 20-d pregnant rats during the OGGT; B, area under the curve for glucose of control (*gray bar*) and englitazone-treated (*black bar*) 20-d pregnant rats during the OGGT; C, plasma insulin of control (*gray circles*) and englitazone-treated (*black circles*) 20-d pregnant rats during the OGGT; D, area under the curve for insulin of control (*gray bar*) and englitazone-treated (*black bar*) 20-d pregnant rats during the OGGT. *, $P < 0.05$, englitazone-treated *vs.* untreated control animals.

IRS-1, IRS-2, PI3K, PDK-1, Akt/PKB, ERK1/2, and PTEN in response to the drug. As discussed above, our data point to the involvement of IRS-1 serine 307 phosphorylation in the insulin-resistant condition of adipose tissue in late pregnancy. This would imply that the antidiabetic action of en-

glitazone during gestation should be reflected in a reduction of IRS-1 phosphorylation at serine 307. In line with this hypothesis, we found that englitazone-treated pregnant rats had significantly lower levels of serine 307-phosphorylated IRS-1 in lumbar adipose tissue than untreated control animals (Fig. 5B). These findings therefore indicate that the treatment of pregnant rats with the antidiabetic drug apparently reverses the impairment of IRS-1 signaling by restoring the dephosphorylated state of serine 307 and that this reversal correlates with the improvement of insulin responsiveness. Together, these data support a role for enhanced serine 307 phosphorylation of IRS-1 in the development of adipose tissue insulin resistance at late pregnancy and suggest that this modification of IRS-1 is relevant to the pharmacological treatment of insulin resistance with TZDs. This is also supported by previous studies showing that TZDs potentiate insulin-stimulated PI3K and Akt activation in cultured cells (40), that long-term treatment with troglitazone increases insulin-stimulated Akt phosphorylation in skeletal muscle (38), and that the TZD rosiglitazone interferes with serine phosphorylation of IRS-1 *in vitro* and in an animal model of obesity (34).

Pharmacological restoration of insulin responsiveness and serine 307 dephosphorylation of IRS-1 in adipose tissue are accompanied by an increase of circulating and tissue adiponectin

Different mechanisms might account for the ability of englitazone to reduce IRS-1 serine phosphorylation and promote insulin sensitization in adipose tissue at late pregnancy. First, at the molecular level, pharmacological activation of PPARγ by TZD causes body-wide lipid redistribution, lowering free fatty acids and triglyceride in the circulation and thereby improving insulin sensitivity (41). Second, PPARγ agonists stimulate the production of adiponectin, a highly expressed protein in white adipose tissue and one of the most abundant plasma proteins (42). Adiponectin promotes fatty acid oxidation and insulin sensitivity (43). In fact, hypoadiponectinemia is a hallmark of conditions of insulin resistance, including obesity (44), type 2 diabetes (45), and gestational diabetes (46). Furthermore, a low maternal plasma adiponectin concentration has been found to be an independent predictor of gestational diabetes (47). Recently, it has been shown that late pregnancy in humans is associated with a significant decrease in adiponectin both in plasma (48) and in adipose tissue (49). Moreover, the observed reductions in adiponectin levels correlate with decreased insulin sensitivity of glucose disposal in muscle during pregnancy (49). Interestingly, a very recent study shows that adiponectin sensitizes insulin signaling by reducing p70 S6 kinase-mediated serine phosphorylation of IRS-1 (50). According to this observation, it is tempting to speculate that the observed decrease of IRS-1 serine 307 phosphorylation in adipose tissue of englitazone-treated pregnant rats (see above) may be related to an increase of adiponectin. In agreement with this possibility, we found that circulating adiponectin levels were significantly higher in englitazone-treated pregnant rats than in control animals (Table 2), being similar to those detected in the nonpregnant condition (Table 1). We further analyzed adiponectin expression in adipose tissue of these animals. As

shown in Fig. 6, adiponectin was significantly decreased at late pregnancy ($P < 0.05$). Treatment with englitazone markedly augmented the amount of the adipokine ($P < 0.001$) to levels that were even higher than in the nonpregnant condition ($P < 0.001$). These data demonstrate that englitazone reverses the decrease of both circulating and tissue adiponectin at late pregnancy and support the role of decreased adiponectin levels in the low responsiveness of adipose tissue to insulin during late pregnancy. However, it has been suggested that changes in systemic adiponectin specifically predicts the reduced insulin sensitivity for glucose but not for lipid metabolism in human pregnancy (49).

Impaired insulin-stimulated tyrosine phosphorylation of IRS-1 in adipose tissue of late pregnant rats can be restored ex vivo by treating isolated adipocytes with adiponectin

In adipose tissue of virgin rats, insulin increased tyrosine phosphorylation of IRS-1 about 4-fold, whereas in pregnant animals, the stimulatory effect of insulin was approximately 2-fold (see Fig. 1C). As discussed above, decreased adiponectin levels during pregnancy might account for such an impaired response to insulin. To substantiate this hypothesis, we investigated whether the insulin-stimulated tyrosine phosphorylation of IRS-1 in adipose tissue of pregnant rats could be restored *ex vivo* upon treatment of isolated adipocytes with adiponectin. As shown in Fig. 7, insulin-stimulated tyrosine phosphorylation of IRS-1 in adipocytes from
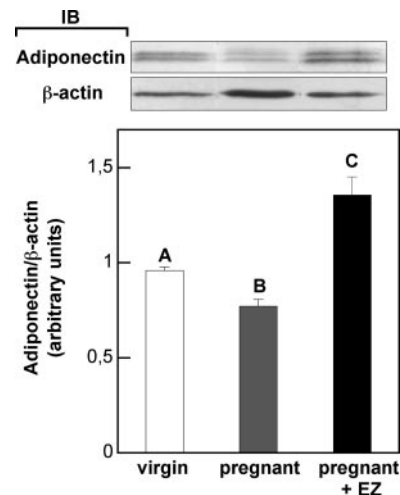

FIG. 6. Decreased adipose tissue adiponectin levels at late pregnancy are normalized by englitazone treatment. Adipose tissue from nonpregnant (*white bar*) and 20-d pregnant rats treated with saline (*gray bar*) or englitazone (*black bar*) was homogenized in an ice-cold 30 mM HEPES buffer (pH 7.4), containing 5 mM EDTA, 1% Triton X-100, 0.5% sodium deoxycholate, and 2 mM protease inhibitor (Pefablock). Western blot analysis of adiponectin reveals that at late pregnancy the amount of the adipokine in adipose tissue is decreased and that englitazone (EZ) treatment augmented the amount of the adipokine to levels even higher than in the nonpregnant condition. The graph shows the levels of adiponectin, normalized to β-actin, of virgin (n = 5), control 20-d pregnant (n = 8), and englitazone-treated (n = 6) 20-d pregnant rats. A representative immunoblot (IB) for adiponectin and β-actin is shown above the graph. Statistical analysis was performed by ANOVA followed by Student-Newman Keuls *post hoc* test. Significance is shown by *letters*: *different letters* indicate significant differences ($P < 0.05$) between the groups.
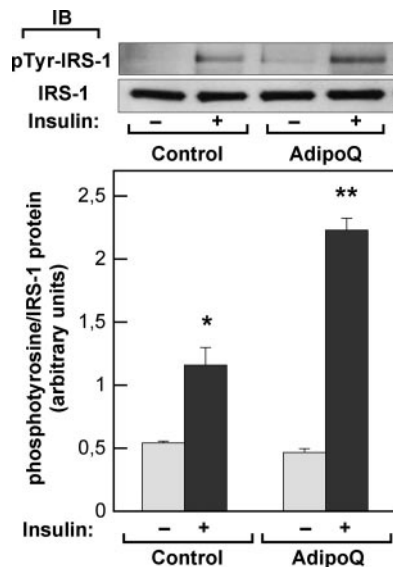
FIG. 7. Adiponectin (AdipoQ) enhances the impaired insulin-stimulated tyrosine phosphorylation of IRS-1 in adipocytes from late pregnant rats. Adipocytes isolated from lumbar adipose tissue of 20-d pregnant rats were incubated in KRB buffer for 30 min in the absence or presence of 1 μg/ml recombinant AdipoQ. Subsequently, cells were incubated for another 5 min in the absence (*light gray bars*) and presence (*dark gray bars*) of 100 nM insulin. Protein extracts were obtained by lysis of the cells in RIPA buffer containing 30 mM HEPES (pH 7.4), 5 mM EDTA, 1% Nonidet P-40, 1% Triton X-100, 0.5% sodium deoxycholate, 8 mM Na_3VO_4, 1 mM NaF, and 2 mM protease inhibitor (Pefablock) and subjected to Western blot analysis for anti-phospho-IRS-1 (Tyr612) and anti-IRS-1. The graphs show the level of tyrosine-phosphorylated IRS-1 normalized to the total amount of IRS-1 in each sample. Representative immunoblots (IB) for phosphorylated and total IRS-1 are shown above the graph. *, $P < 0.05$; **, $P < 0.01$, 100 *vs.* 0 nM insulin.

pregnant rats was only 2.15 ± 0.13-fold. In the presence of adiponectin, this response to insulin was significantly ($P = 0.003$) enhanced as evidenced by a 4.78 ± 0.08-fold increase of IRS-1 tyrosine phosphorylation. These data further support the hypothesis that decreased adiponectin levels might account at least partially for impaired insulin signaling at late gestation.

Although our findings point to role for adiponectin in the modulation of insulin signaling in adipose tissue of pregnant rats, we cannot discard that other potential mediators could be implicated in the initiation of insulin resistance during pregnancy. Pregnancy can be considered a condition of moderate inflammation (51, 52), in which adipose tissue together with placenta contributes to the local and systemic increase of inflammatory molecules such as TNF-α, leptin, IL-1β, IL-6, IL-10, monocyte chemotactic protein 1 (MCP-1), and resistin (53). The physiological role of this low-grade inflammation is uncertain. It has been proposed that activation of some inflammatory pathways is implicated in the development of insulin resistance at late pregnancy and that when this physiological adaptation is decompensated, the mother is at a major risk of gestational diabetes (54). Indeed, it has been shown in human pregnancy that circulating concentrations of TNF-α correlate significantly with insulin resistance (55). Thus, we speculate that inflammatory molecules, via activation of Ser/Thr kinases, together with low adiponectin

levels, could be implicated in the development of insulin resistance during pregnancy.

In conclusion, here we present experimental data that support a role for increased serine 307 phosphorylation of IRS-1, paralleled by a reduction of circulating and tissue adiponectin, in the modulation of insulin resistance in adipose tissue during late pregnancy. We anticipate that the identification of the protein kinases involved in IRS-1 serine phosphorylation, as well as future studies on the regulation of these kinases by circulating mediators such as adiponectin, will provide novel targets for pharmacological interventions designed to reduce the risk of adverse outcomes related to exaggerated insulin resistance in pregnancy, which is the main responsible factor for the development of gestational diabetes in women.

Acknowledgments

References

1. **Ryan EA, O'Sullivan MJ, Skyler JS** 1985 Insulin action during pregnancy. Studies with the euglycemic clamp technique. Diabetes 34:380–389
2. **Catalano PM, Tyzbir ED, Wolfe RR, Calles J, Roman NM, Amini SB, Sims EA** 1993 Carbohydrate metabolism during pregnancy in control subjects and women with gestational diabetes. Am J Physiol 264:E60–E67
3. **Buchanan TA, Metzger BE, Freinkel N, Bergman RN** 1990 Insulin sensitivity and B-cell responsiveness to glucose during late pregnancy in lean and moderately obese women with normal glucose tolerance or mild gestational diabetes. Am J Obstet Gynecol 162:1008–1014
4. **Leturque A, Ferrè P, Burnol A-F, Kande J, Maulard P, Girard J** 1986 Glucose utilization rates and insulin sensitivity in vivo in tissues of virgin and pregnant rats. Diabetes 35:172–177
5. **Ramos P, Herrera E** 1995 Reversion of insulin resistance in the rat during late pregnancy by 72-h glucose infusion. Am J Physiol 269:E858–E863
6. **Ramos P, Herrera E** 1996 Comparative responsiveness to prolonged hyperinsulinemia between adipose-tissue and mammary-gland lipoprotein lipase activities in pregnant rats. Early Pregnancy 2:29–35
7. **Ramos MP, Crespo-Solans MD, del Campo S, Cacho J, Herrera E** 2003 Fat accumulation in the rat during early pregnancy is modulated by enhanced insulin responsiveness. Am J Physiol Endocrinol Metab 285:E318–328
8. **Virkamäki A, Ueki K, Kahn CR** 1999 Protein-protein interaction in insulin signaling and the molecular mechanisms of insulin resistance. J Clin Invest 103:931–943
9. **Shepherd PR, Withers DJ, Siddle K** 1998 Phosphoinositide 3-kinase: the key switch mechanism in insulin signalling. Biochem J 333:471–490
10. **Saltiel AR, Kahn CR** 2001 Insulin signalling and the regulation of glucose and lipid metabolism. Nature 414:799–806
11. **Hill MM, Clark SF, Tucker DF, Birnbaum MJ, James DE, Macaulay SL** 1999 A role for protein kinase Bβ/Akt2 in insulin-stimulated GLUT4 translocation in adipocytes. Mol Cell Biol 19:7771–7781
12. **Foran PG, Fletcher LM, Oatey PB, Mohammed N, Dolly JO, Tavare JM** 1999 Protein kinase B stimulates the translocation of GLUT4 but not GLUT1 or transferrin receptors in 3T3-L1 adipocytes by a pathway involving SNAP-23, synaptobrevin-2, and/or cellubrevin. J Biol Chem 274:28087–28095
13. **Le Roith D, Zick Y** 2001 Recent advances in our understanding of insulin action and insulin resistance. Diabetes Care 24:588–597
14. **Paz K, Hemi R, LeRoith D, Karasik A, Elhanany E, Kanety H, Zick Y** 1997 A molecular basis for insulin resistance. Elevated serine/threonine phosphorylation of IRS-1 and IRS-2 inhibits their binding to the juxtamembrane region of the insulin receptor and impairs their ability to undergo insulin-induced tyrosine phosphorylation. J Biol Chem 272:29911–29918

15. **Zick Y** 2001 Insulin resistance: a phosphorylation-based uncoupling of insulin signaling. Trends Cell Biol 11:437–441
16. **Rui L, Aguirre V, Kim JK, Shulman GI, Lee A, Corbould A, Dunaif A, White MF** 2001 Insulin/IGF-1 and TNF-α stimulate phosphorylation of IRS-1 at inhibitory Ser307 via distinct pathways. J Clin Invest 107:181–189
17. **Delahaye L, Mothe-Satney I, Myers MG, White MF, Van Obberghen E** 1998 Interaction of insulin receptor substrate-1 (IRS-1) with phosphatidylinositol 3-kinase: effect of substitution of serine for alanine in potential IRS-1 serine phosphorylation sites. Endocrinology 139:4911–4919
18. **Sutter-Dub MT, Sfaxi A, Latrille F, Sodoyez-Goffaux F, Sodoyez JC** 1984 Insulin binding and action in adipocytes of pregnant rats: evidence that insulin resistance is caused by post-receptor binding defects. J Endocrinol 102:209–214
19. **Flint DJ, Sinnett-Smith PA, Clegg RA, Vernon RG** 1979 Role of insulin receptors in the changing metabolism of adipose tissue during pregnancy and lactation in the rat. Biochem J 182:421–427
20. **Gonzalez CG, Alonso A, Balbin M, Diaz F, Fernandez S, Patterson AM** 2002 Effects of pregnancy on insulin receptor in liver, skeletal muscle and adipose tissue of rats. Gynecol Endocrinol 16:193–205
21. **Saad MJA, Maeda L, Brenelli SL, Carvalho CRO, Paiva RS, Velloso LA** 1997 Defects in insulin signal transduction in liver and muscle of pregnant rats. Diabetologia 40:179–186
22. **Friedman JE, Ishizuka T, Shao J, Huston L, Highman T, Catalano P** 1999 Impaired glucose transport and insulin receptor tyrosine phosphorylation in skeletal muscle from obese women with gestational diabetes. Diabetes 48:1807–1814
23. **Catalano PM, Nizielski SE, Shao J, Preston L, Qiao L, Friedman JE** 2002 Downregulated IRS-1 and PPARgamma in obese women with gestational diabetes: relationship to FFA during pregnancy. Am J Physiol Endocrinol Metab 282:E522–E533
24. **Kahn BB, Flier JS** 2000 Obesity and insulin resistance. J Clin Invest 106:473–481
25. **Matthews DR, Hosker JP, Rudenski AS, Naylor BA, Treacher DF, Turner RC** 1985 Homeostasis model assessment: insulin resistance and β-cell function from fasting plasma glucose and insulin concentrations in man. Diabetologia 28:412–419
26. **Katz A, Nambi SS, Mather K, Baron AD, Follmann DA, Sullivan G, Quon MJ** 2000 Quantitative insulin sensitivity check index: a simple, accurate method for assessing insulin sensitivity in humans. J Clin Endocrinol Metab 85:2402–2410
27. **Legro RS, Finegood D, Dunaif A** 1998 A fasting glucose to insulin ratio is a useful measure of insulin sensitivity in women with polycystic ovary syndrome. J Clin Endocrinol Metab 83:2694–2698
28. **Chaves JM, Herrera E** 1980 In vitro response of glycerol metabolism to insulin and adrenaline in adipose tissue from fed and fasted rats during pregnancy. Biol Neonate 38:139–145
29. **Herrera E, Munoz C, Lopez-Luna P, Ramos P** 1994 Carbohydrate-lipid interactions during gestation and their control by insulin. Braz J Med Biol Res 27:2499–2519
30. **Carrascosa JM, Ramos P, Molero JC, Herrera E** 1998 Changes in the kinase activity of the insulin receptor account for an increased insulin sensitivity of mammary gland in late pregnancy. Endocrinology 139:520–526
31. **Kellerer M, Lammers R, Haring HU** 1999 Insulin signal transduction: possible mechanisms for insulin resistance. Exp Clin Endocrinol Diabetes 107:97–106
32. **Asante-Appiah E, Kennedy BP** 2003 Protein tyrosine phosphatases: the quest for negative regulators of insulin action. Am J Physiol Endocrinol Metab 284:E663–E670
33. **Hotamisligil GS, Peraldi P, Budavari A, Ellis R, White MF, Spiegelman BM** 1996 IRS-1-mediated inhibition of insulin receptor tyrosine kinase activity in TNF-α- and obesity-induced insulin resistance. Science 271:665–668
34. **Jiang G, Dallas-Yang Q, Biswas S, Li Z, Zhang BB** 2004 Rosiglitazone, an agonist of peroxisome-proliferator-activated receptor γ (PPARγ), decreases inhibitory serine phosphorylation of IRS1 in vitro and in vivo. Biochem J 377:339–346
35. **Zick Y** 2004 Uncoupling insulin signalling by serine/threonine phosphorylation: a molecular basis for insulin resistance. Biochem Soc Trans 32:812–816
36. **White MF** 2006 Regulating insulin signaling and β-cell function through IRS proteins. Can J Physiol Pharmacol 84:725–737
37. **Kintscher U, Law RE** 2005 PPARγ-mediated insulin sensitization: the importance of fat versus muscle. Am J Physiol Endocrinol Metab 288:E287–E291
38. **Meyer MM, Levin K, Grimmsmann T, Perwitz N, Eirich A, Beck-Nielsen H, Klein HH** 2002 Troglitazone treatment increases protein kinase B phosphorylation in skeletal muscle of normoglycemic subjects at risk for the development of type 2 diabetes. Diabetes 51:2691–2697
39. **Smith U, Gogg S, Johansson A, Olausson T, Rotter V, Svalstedt B** 2001 Thiazolidinediones (PPARγ agonists) but not PPARα agonists increase IRS-2 gene expression in 3T3-L1 and human adipocytes. FASEB J 15:215–220
40. **Zhang B, Szalkowski D, Diaz E, Hayes N, Smith R, Berger J** 1994 Potentiation of insulin stimulation of phosphatidylinositol 3-kinase by thiazolidinedione-derived antidiabetic agents in Chinese hamster ovary cells expressing human insulin receptors and L6 myotubes. J Biol Chem 269:25735–25741
41. **Evans RM, Barish GD, Wang YX** 2004 PPARs and the complex journey to obesity. Nat Med 10:355–361
42. **Trujillo ME, Scherer PE** 2005 Adiponectin: journey from an adipocyte secretory protein to biomarker of the metabolic syndrome. J Intern Med 257:167–175
43. **Yamauchi T, Kamon J, Waki H, Terauchi Y, Kubota N, Hara K, Mori Y, Ide T, Murakami K, Tsuboyama-Kasaoka N, Ezaki O, Akanuma Y, Gavrilova O, Vinson C, Reitman ML, Kagechika H, Shudo K, Yoda M, Nakano Y, Tobe K, Nagai R, Kimura S, Tomita M, Froguel P, Kadowaki T** 2001 The fat-derived hormone adiponectin reverses insulin resistance associated with both lipoatrophy and obesity. Nat Med 7:941–946
44. **Hu E, Liang P, Spiegelman BM** 1996 AdipoQ is a novel adipose-specific gene dysregulated in obesity. J Biol Chem 271:10697–10703
45. **Statnick MA, Beavers LS, Conner LJ, Corominola H, Johnson D, Hammond CD, Rafaeloff-Phail R, Seng T, Suter TM, Sluka JP, Ravussin E, Gadski RA, Caro JF** 2000 Decreased expression of apM1 in omental and subcutaneous adipose tissue of humans with type 2 diabetes. Int J Exp Diabetes Res 1:81–88
46. **Worda C, Leipold H, Gruber C, Kautzky-Willer A, Knofler M, Bancher-Todesca D** 2004 Decreased plasma adiponectin concentrations in women with gestational diabetes mellitus. Am J Obstet Gynecol 191:2120–2124
47. **Weerakiet S, Lertnarkorn K, Panburana P, Pitakitronakorn S, Vesathada K, Wansumrith S** 2006 Can adiponectin predict gestational diabetes? Gynecol Endocrinol 22:362–368
48. **Fuglsang J, Skjaerbaek C, Frystyk J, Flyvbjerg A, Ovesen P** 2006 A longitudinal study of serum adiponectin during normal pregnancy. BJOG 113:110–113
49. **Catalano PM, Hoegh M, Minium J, Huston-Presley L, Bernard S, Kalhan S, Hauguel-De Mouzon S** 2006 Adiponectin in human pregnancy: implications for regulation of glucose and lipid metabolism. Diabetologia 49:1677–1685
50. **Wang C, Mao X, Wang L, Liu M, Wetzel MD, Guan KL, Dong LQ, Liu F** 2007 Adiponectin sensitizes insulin signaling by reducing p70 S6 kinase-mediated serine phosphorylation of IRS-1. J Biol Chem 282:7991–7996
51. **Faas MM, Schuiling GA, Linton EA, Sargent IL, Redman CW** 2000 Activation of peripheral leukocytes in rat pregnancy and experimental preeclampsia. Am J Obstet Gynecol 182:351–357
52. **von Dadelszen P, Wilkins T, Redman CW** 1999 Maternal peripheral blood leukocytes in normal and pre-eclamptic pregnancies. Br J Obstet Gynaecol 106:576–581
53. **Hauguel-de Mouzon S, Guerre-Millo M** 2006 The placenta cytokine network and inflammatory signals. Placenta 27:794–798
54. **Di Benedetto A, Russo GT, Corrado F, Di Cesare E, Alessi E, Nicocia G, D'Anna R, Cucinotta D** 2005 Inflammatory markers in women with a recent history of gestational diabetes mellitus. J Endocrinol Invest 28:34–38
55. **Kirwan JP, Hauguel-De Mouzon S, Lepercq J, Challier JC, Huston-Presley L, Friedman JE, Kalhan SC, Catalano PM** 2002 TNF-α is a predictor of insulin resistance in human pregnancy. Diabetes 51:2207–2213